Shock-wave compression and tension of solids at elevated temperatures: superheated crystal states, pre-melting, and anomalous growth of the yield strength

2004 J. Phys.: Condens. Matter 16 S1007

(http://iopscience.iop.org/0953-8984/16/14/010)

INSTITUTE OF PHYSICS PUBLISHING JOURNAL OF PHYSICS: CONDENSED MATTER

J. Phys.: Condens. Matter **16** (2004) S1007–S1016 PII: S0953-8984(04)74825-0

Shock-wave compression and tension of solids at elevated temperatures: superheated crystal states, pre-melting, and anomalous growth of the yield strength

G I Kanel, S V Razorenov and V E Fortov

Institute for High Energy Densities of Russian Academy of Sciences, IVTAN, Izhorskaya 13/19, Moscow, 125412, Russia

Received 20 January 2004
Published 26 March 2004
Online at stacks.iop.org/JPhysCM/16/S1007
DOI: 10.1088/0953-8984/16/14/010

Abstract

Recent studies of the response of metals and alloys to shock-wave loading at elevated temperatures are summarized. Shock-wave tests have been carried out for metal single crystals, polycrystalline metals of different purity, and for alloys. High resistance to sub-microsecond tensile fracture of single crystals is maintained when melting should start. This is treated as evidence of a superheated solid state reached under dynamic tension. In polycrystalline metals, melting starts earlier at grain boundaries; this is known as the pre-melting phenomenon. As a result, their tensile strength drops to zero on approaching the melting curve. Anomalous growth of the dynamic yield stress was observed for low-strength metals, whereas the yield stress of high-strength alloys decreases with temperature. The different behaviour of metals and alloys is treated in terms of the relationship between the phonon drag of the motion of dislocations and the drag forces created by obstacles.

1. Introduction

In addition to high pressures and temperatures, the compression of materials by strong shock waves is associated with extremely high rates of variation of these quantities. This circumstance opens unique opportunities for the generation and study of metastable states and non-equilibrium processes in a matter. A high rate of load application may lead to the activation of new mechanisms of deformation and fracture. Introducing the temperature as a variable parameter in shock wave experiments much extends this area of investigations.

Expected temperature effects upon the elastic–plastic and strength properties of solids at very high strain rates are not trivial and are not yet entirely clear. It is well known that, under normal conditions, both the yield strength and the tensile strength of materials are strong

functions of temperature and decrease with heating. For low rates of mechanical loading, the dislocation motion is aided by thermal fluctuations. Dislocation motion is impeded at barriers and a combination of thermal agitation and applied stress is required to activate dislocations over the obstacles [1]. In order to provide high rates of deformation (10^4–10^5 s^{-1} and more) one should apply such stresses that are high enough to overcome instantaneously the usual dislocation barriers without any aid from thermal fluctuations. Under these conditions, viscous phonon drag may become dominant in the resistance to motion of dislocations. Since the phonon drag is proportional to the temperature, an anomalous increase of the flow stress with increasing temperature may be expected at the highest strain rates. Atomistic simulations of the dislocation motion show that the dislocation velocity decreases with increasing temperature and confirm that the drag is due to thermal phonons [2]. On the other hand, thermal fluctuations provide a mechanism of homogeneous nucleation of dislocations [3] and in this way should decrease the flow stress.

A possible influence of the temperature upon the bulk tensile strength of materials at very high strain rates is also complicated. As a result of over-stressing, the fracture process becomes scattered in nature and consists of nucleation, growth, and coalescence of numerous pores or cracks [4]. Temperature may obviously influence the nucleation and growth processes. Spontaneous nucleation of microvoids by thermal fluctuations should decrease the strength. On the other hand, the resistance to growth of pores is determined by the yield stress and by the viscosity of the surrounding material, so it has to change with the temperature proportionally to the change of flow stress. If the flow stress increases with temperature as a result of phonon drag at high strain rates, the total resistance to fracture should also increase. The influence of melting under tension on the resistance to fracture is a question of especial interest.

Recent studies [5–8] of the response of polycrystalline metals and metal single crystals to shock wave loading have shown their unusual behaviour at elevated temperatures and strain rates of $>10^5$ s^{-1}. It was found that the resistance to high-rate tensile fracture of metals does not vary much on increasing the temperature at least up to 85–90% of the absolute melting temperature, T_m. With further temperature increase, a different behaviour of the strength was observed, depending on the material structure. Whereas polycrystalline metals exhibit a precipitous decrease of strength down to practically zero as soon as the temperature approaches T_m, the dynamic tensile strength of single crystals remains high even in the close vicinity of T_m. The dynamic yield stress in some cases increases with heating or it may be independent of the temperature.

In order to understand in which cases anomalous growth of yield stress with heating may occur and what governs the resistance to fracture at elevated temperatures, it would be desirable to compare the behaviour of different metals and alloys. Besides analysing the governing mechanisms of plastic deformation and fracture at the highest strain rates, investigations of the strength properties of alloys are important from a practical point of view. In this paper we present new experimental data for metals and alloys, which may contribute in understanding the mechanisms of deformation and fracture at very high strain rates.

2. The method

In the experiments, one-dimensional shock loads were created in the samples by impacts of flyer plates launched with explosive facilities or with a gas gun. Using plane impactors of different thickness the shock load duration was varied, whereas the impact velocity controlled the peak shock stress [9]. Dynamic yielding and spall fracture appear in the structure of compression and rarefaction waves, and are recorded by monitoring the free surface velocity histories with a VISAR laser Doppler velocimeter [10].

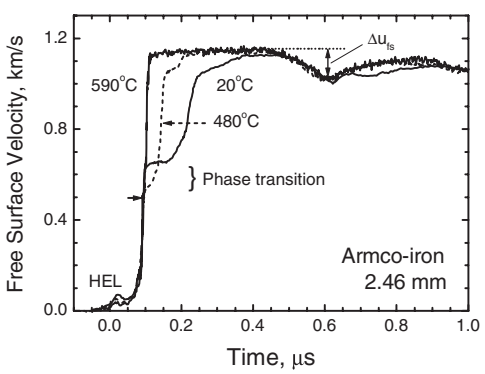

Figure 1. Free surface velocity histories of Armco iron plates 2.46 mm in thickness impacted by aluminium flyer plates 2 mm thick at normal and elevated temperatures. The impact velocity was 1.9 ± 0.05 km s^{-1}.

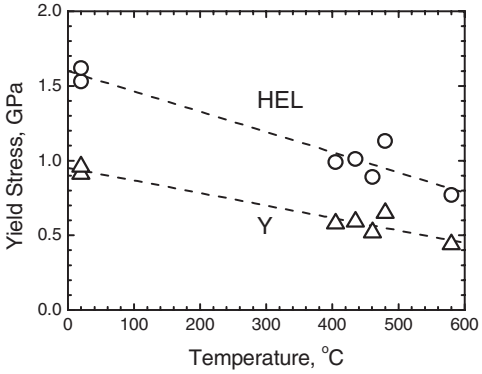

Figure 2. Temperature dependences of the Hugoniot elastic limit (HEL) and corresponding yield stress for Armco iron.

Figure 1 presents examples of such tests for Armco iron. As a result of different longitudinal compressibilities at stresses below the Hugoniot elastic limit (HEL) and above it, the shock wave becomes unstable and is split into an elastic precursor wave, which propagates with the longitudinal elastic wave speed, and a plastic shock wave with a lower propagation velocity. The peak stress behind the elastic precursor front is

$$\sigma_{\mathrm{HEL}} = (1-\nu)Y/(1-2\nu) = (2/3)Y_{\mathrm{c}}/(1-c_{\mathrm{b}}^2/c_{\mathrm{l}}^2) = (1/2)(c_{\mathrm{l}}/c_{\mathrm{s}})^2 \qquad (1)$$

where Y is the yield stress of the material measured under one-dimensional stress conditions, ν is Poisson's ratio, c_{l}, c_{s}, c_{b} are longitudinal, shear, and bulk sound velocities respectively, and the compressive stress is assumed positive. Figure 2 shows the dynamic yielding data for Armco iron, which have been determined from measured free surface velocity histories. Since the temperature was varied, the dependences of Poisson's ratio and sound speeds upon temperature were accounted for in these calculations.

It is known that the $\alpha \rightarrow \varepsilon$ phase transition occurs in iron under compression. The change in the crystal structure is accompanied by a change in compressibility, which, in turn, results in splitting of plastic shock waves. The state behind the first plastic shock wave of the two-shock configuration is the state at the beginning of the polymorphic transformation into the high-pressure phase. The wave profiles in figure 1 demonstrate the decrease of the transformation pressure with increasing temperature.

When a compression pulse is reflected from the body free surface, the interaction of two rarefaction waves produces tensile stresses inside the body that cause a tensile fracture. This kind of dynamic fracture is called 'spall fracture' or 'spallation'. The velocity pullback Δu_{fs} is a measure of incipient fracture strength, σ^*, of the material:

$$\sigma^* = \tfrac{1}{2}\rho_0 c_{\mathrm{b}}(\Delta u_{\mathrm{fs}} + \delta), \qquad (2)$$

where δ is a correction for distortion of the waveform due to the elastic–plastic properties of the material [11].

3. Dynamic strength properties near the melting temperature

Figures 3 and 4 show the spall strength dependences on the test temperature for zinc [6] and aluminium [7] single crystals and for polycrystalline aluminium AD1 and magnesium

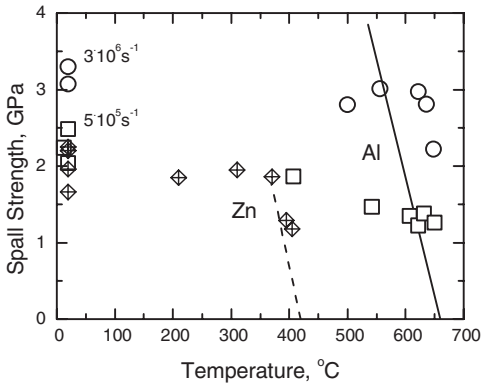

Figure 3. The relationship between spall strength (points) and melting thresholds (lines) for zinc and single crystals of aluminium at two different strain rates.

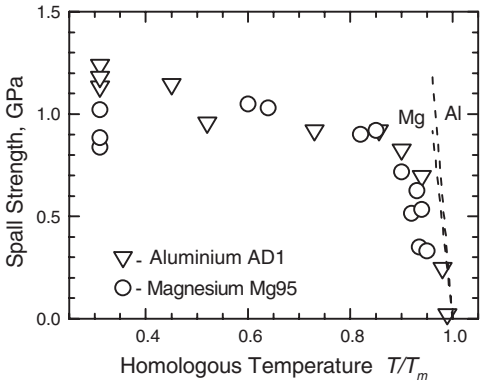

Figure 4. The relationship between spall strength and melting thresholds for polycrystalline aluminium and magnesium. T_{m} is the melting temperature in kelvins.

Mg95 [5]. The figures also show linear estimations of the pressure at which the isentrope of a solid intersects the melting curve under tension. It can be shown [11] that the intersection point is given by the equation

$$p\alpha \frac{\mathrm{d}T_{\mathrm{m}}}{\mathrm{d}p} - \frac{p}{K_{\mathrm{T}}} = \alpha(T_0 - T_{\mathrm{m}0}) - \frac{p}{K_S} \tag{3}$$

where α is the thermal expansion coefficient, T_0 is the initial test temperature, and K_{T} and K_S are the isothermal and the isentropic bulk modules, respectively. All states of condensed matter at negative pressures are below the sublimation curve and are metastable with respect to two separate pieces of the material or to mixtures of the condensed and vapour phases. From this point of view, melting under tension, if it is observed, is a transformation of a metastable solid phase into a metastable liquid phase. On the other hand, equality of the Gibbs potentials of metastable solid and liquid phases at the same pressure and temperature means that the phases are in equilibrium. In this sense, states on the phase boundary are in equilibrium even at negative pressures.

When the pressure in states of tension intersects the melting boundary, the solid states cease to be thermodynamically stable and melting should start. It would be natural to expect a sharp decrease in tensile strength with the beginning of melting. As a result, the lines in figures 3 and 4 should describe melting thresholds, which limit the high-temperature strength of the metals. However, whereas all experimental data for polycrystalline metals are below the estimated melting lines, part of the high-temperature data for single crystals is above these lines. In other words, the strength of polycrystalline metals drops when the material begins to melt, whereas single crystals maintain a high resistance to spall fracture even above the point at which melting should start.

In polycrystalline solids, melting may start along grain boundaries at temperatures below the melting temperature of the crystal. The effect is caused by the disorder and by the larger concentration of impurities in boundary layers of grains [12, 13]. Several computational works have been devoted to detailed study of the role of intergranular surfaces in the melting process at temperatures below the bulk melting point. In particular, Lu and Szpunar [14] have found that partial melting of the grain boundary in aluminium had occurred at temperatures above $0.94T_{\mathrm{m}}$. Very likely, this grain-boundary effect contributed to the precipitous drop in spall strength near, but below, the melting temperature.

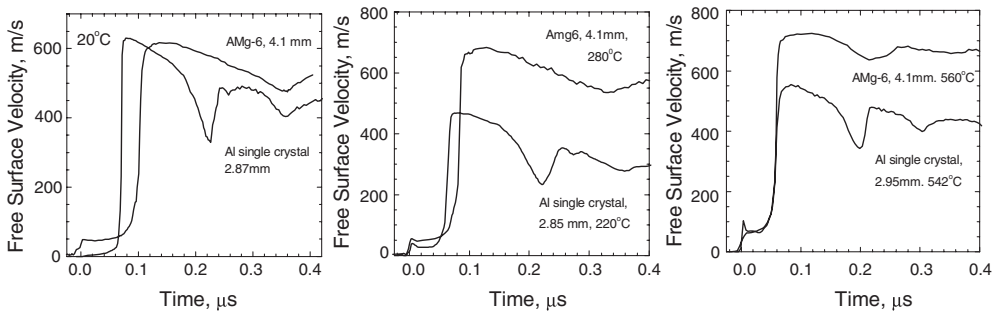

Figure 5. Free surface velocity histories of samples of Al–6% Mg alloy shocked at normal and elevated temperatures in comparison with the data for aluminium single crystals.

If molten spots appear in the volume of a single crystal, the crystal is no longer homogeneous and should show spall strength close to that of the polycrystalline metal. However, even at the highest temperatures, the single crystals demonstrate a higher strength than polycrystalline materials. It seems more likely that the crystals did not melt and the spall data in all cases represent the strength of the solid crystals. If melting did not occur, one has to conclude that superheated solid states were realized in the crystals under tension.

It is known that superheating of crystalline solids is impossible under normal conditions. The crystal surface plays a crucial role because of the very low activation energy of the surface melting. However, superheated states may be reached inside the crystal body if its surface is below the melting temperature. This condition was realized in the spall experiments discussed. The magnitude of superheating of aluminium crystals reached 60–65 °C at the shortest load durations.

Figure 5 compares the free surface velocity histories of aluminium single crystals and Al–6% Mg alloy at normal and elevated temperatures [15]. Unlike Armco iron, the wave profiles for single crystals show significant increase in the precursor wave amplitude with increased temperature. Whereas at room temperature the peak stress in the elastic precursor wave for single crystals is much lower than that for the alloy, they gradually become equal as the temperature increases.

Figure 6 presents the yield stress data for aluminium single crystals and Al–6% Mg alloy. Since Poisson's ratio increases with temperature, the yield stress is less sensitive to the temperature than is the Hugoniot elastic limit. The data show that the dynamic yield stress of pure aluminium crystals increases linearly with increasing temperature. At room temperature the alloy has a shock yield stress that approximately equals that of aluminium crystal at highest temperatures; at 600 °C both materials show practically the same yield stresses.

For the following discussion, let us consider the well known relationship between the resolved shear stress, τ, the plastic shear strain rate, $\dot{\gamma}$, and the mobile dislocation density, N_{m}:

$$\tau = \frac{B}{b^2 N_{\mathrm{m}}}\dot{\gamma}, \tag{4}$$

where b is the Burgers vector, and B is the drag coefficient. The initial density of mobile dislocations, N_{m}, in single crystal samples obviously does not depend on the temperature or, at least, does not decrease with heating. The compressive strain rate in the experiments shown in figure 5 obviously does not increase with increasing temperature. Under these circumstances we have to conclude that the observed increase in the yield stress, Y, and, correspondingly, in the resolved shear stress, τ, is determined by an increase in the drag coefficient B. The over-barrier motion of dislocations is decelerated by various obstacles and by friction forces

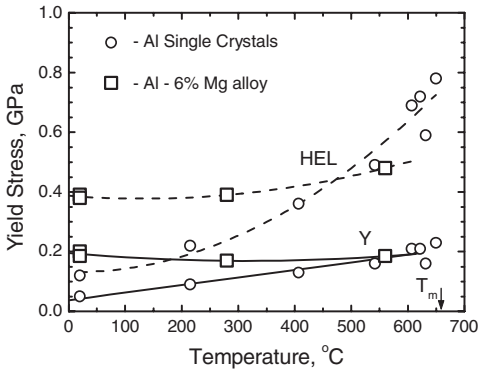

Figure 6. Hugoniot elastic limits and corresponding yield stresses of aluminium single crystals and Al–6% Mg alloy as functions of temperature. T_m is the aluminium melting temperature.

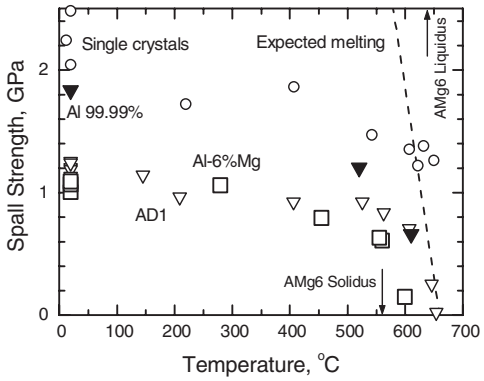

Figure 7. The spall strength of different aluminiums and aluminium alloy as a function of temperature. The data for aluminium of 99.99% purity have been obtained at a higher strain rate than the rest data.

due to phonons. The phonon drag coefficient B_p increases linearly with temperature [16]:

$$B_p = \frac{k_B T \omega_D^2}{\pi^2 c^3}, \tag{5}$$

where k_B is the Boltzmann constant, ω_D is the Debye frequency, and c is the speed of sound. The observed nearly linear increase of the dynamic yield stress with temperature agrees reasonably well with equation (5) for the phonon friction coefficient.

The flow stress in the pure aluminium crystal is small and comparable with the phonon friction forces; therefore growth of the latter makes an essential contribution to the drag of the dislocations. In contrast to pure aluminium, the alloy contains numerous obstacles such as interphase boundaries, inclusions, etc, that have been created specifically to increase the yield strength. At low and moderate temperatures the stress needed to overcome these obstacles far exceeds the forces of phonon drag, which are, therefore, unable to make a significant contribution to the resistance to plastic flow. As the temperature increases, 'thermal strengthening' of the alloy due to growth of the phonon friction forces becomes high enough to compensate its 'softening' due to thermal fluctuations. Thus, the behaviour of the Al–6% Mg alloy is in agreement with the hypothesis that phonon friction is the dominant mechanism at high strain rates and temperatures.

Figure 7 summarizes the results of measurements of the dynamic tensile strength of Al–6% Mg alloy in comparison with similar data for high-purity polycrystalline aluminium, commercial grade aluminium AD1, and aluminium single crystals. The point for the alloy at 600 °C indicates rather an overestimation of the strength; in fact this temperature is above the alloy solidus at which the alloy begins to melt. Regardless of the purity, polycrystalline aluminium loses its strength on approaching the melting temperature. Whereas the alloy and commercial aluminium have practically the same strength at normal and moderate temperatures, partial melting of the alloy at the solidus temperature sharply decreases its strength relative to aluminium.

4. Thermal 'softening' and 'hardening' of titanium and its alloy

The different shock behaviour of pure metals and metal alloys at elevated temperatures was confirmed by experiments with titanium. Figure 8 presents examples of free surface velocity

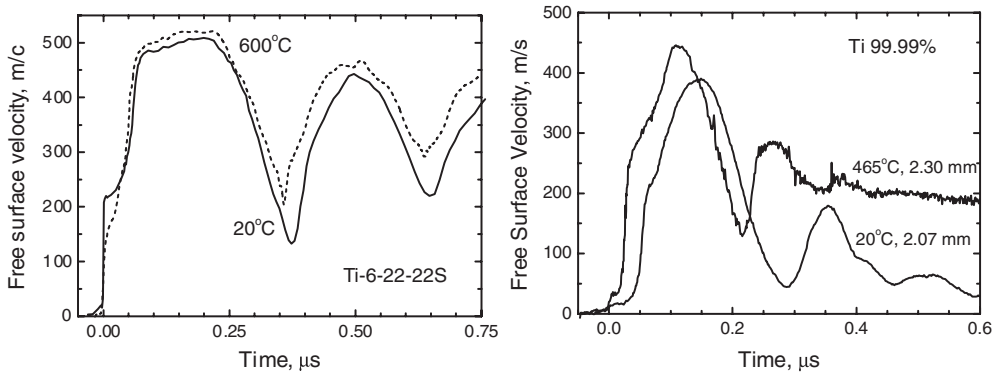

Figure 8. Free surface velocity histories of the Ti-6-22-22S titanium alloy and high-purity titanium samples 2–2.4 mm in thickness at room and elevated temperatures.

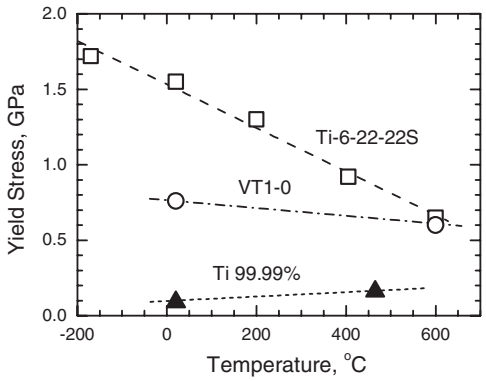

Figure 9. Temperature dependences of dynamic yield strengths of Ti-6-22-22S alloy, commercial grade titanium, and titanium of 99.99% purity.

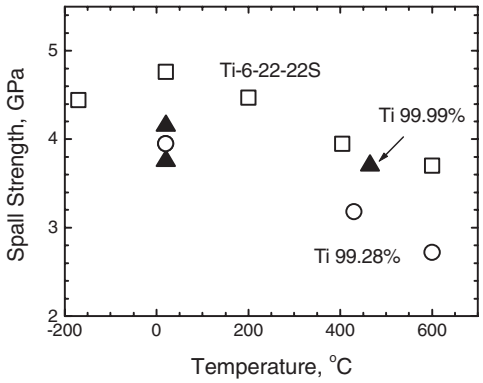

Figure 10. Temperature dependences of the spall strength of Ti-6-22-22S alloy, commercial grade titanium, and titanium of 99.99% purity.

profiles for the α–β titanium alloy Ti-6-22-22S [17] and for α-titanium of high purity [18]. The data demonstrate different signs of the temperature dependences of the Hugoniot elastic limits: whereas the HEL of high-strength alloy decreases with heating it grows abnormally in the case of pure metal.

Figure 9 compares yield strength data for the Ti-6-22-22S alloy, commercial grade titanium VT1-0 of 99.28% purity, and titanium of 99.99% purity. Both the commercial and the high-purity titanium were in the α phase. It is well known that, under normal conditions, the yield stress and tensile strength of titanium increase with increasing the oxygen content (see, for example, [19]). As a result, at room temperature the yield stress of pure titanium is much lower than that of commercial titanium with relatively high oxygen content. However, with increasing temperature this difference decreases. As in the case of aluminium, pure titanium shows an anomalous increase of the yield strength with increasing temperature. Note that the test temperature was far below the melting temperature of titanium. As a result, a possible temperature-dependent contribution of the variable concentration of defects to the drag forces should be insignificant.

The plastic compression wave in pure titanium has a unique feature: namely, the rate of increase of the surface velocity drops abruptly after the velocity reaches about 200 m s^{-1} at

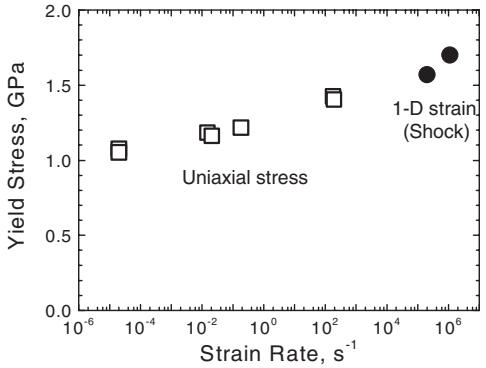

Figure 11. The yield strength at 0.2% plastic strain of Ti-6-22-22S alloy as a function of the strain rate.

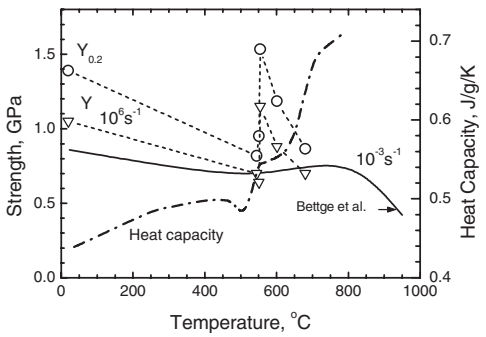

Figure 12. Correlation between anomalies in the yield stress at high-rate shock compression and the heat capacity of Inconel IN 738 LC refractory alloy. Quasi-static yield strength data [22] are shown for comparison.

20 °C or ∼270 m s^{-1} at 465 °C. A similar loss of stability of the shock wave is characteristic of polymorphic transformations with decreasing volume upon compression. Obviously, we detected the known $\alpha \rightarrow \omega$ transformation during compression in our experiments. The values of the transformation pressures are 2.37 GPa at 20 °C and 3.05 GPa at 465 °C. No features possibly to be related to reverse $\omega \rightarrow \alpha$ transformation were detected at the unloading parts of the velocity profiles.

Figure 10 compares the temperature dependences of spall strength data for the titanium alloy, commercial titanium, and pure titanium. Despite the multifold difference in the yield strength, the dynamic strength values do not differ very much for these materials. In the case of pure titanium, the temperature dependence of the dynamic yield strength and tensile strength does not agree even in its signs. As is the case for aluminium alloys, there is no correlation between the sub-microsecond yield strength and the spall strength of titanium and titanium alloys.

Figure 11 summarizes the room-temperature yield strength data evaluated from shock-wave tests under uniaxial strain conditions and from uniaxial stress Hopkinson bar tests at lower strain rates. The yield stresses at 0.2% plastic deformation are plotted because it is difficult to determine precisely the initial Y values from the Hopkinson bar tests. The strain-rate and the temperature dependences of the yield stress obtained from the uniaxial stress tests and from the shock-wave experiments are in good agreement, and demonstrate, in general, a logarithmic dependence over the strain rate range of 10^{-4}–10^{6} s^{-1}. This indicates that the thermal activation mechanism of plastic deformation of the alloy is maintained.

5. Sub-microsecond strength properties of nickel-based refractory superalloy

It may be assumed that both the yield stress and the tensile strength of high-strength alloys decrease monotonically with heating and increase with increasing strain rate. However, the response of complicated materials may not necessarily follow this common trend. Figures 12 and 13 show the temperature dependences of the dynamic yield strength and the spall strength of Inconel IN 738 LC alloy [20]. Inconel is a nickel-based superalloy used as turbine-blade material. The alloy consists of an fcc γ-phase matrix with a high volume fraction of embedded γ' particles. The strengthening precipitates have a long-range-ordered structure with suitable

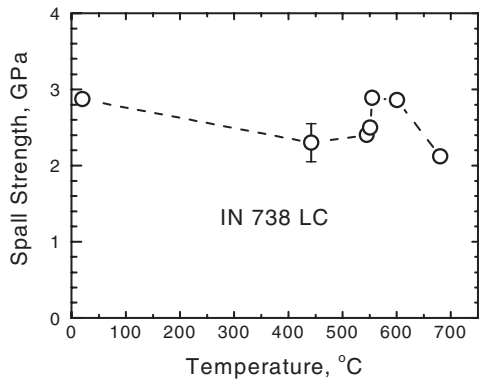

Figure 13. The temperature dependence of spall strength for Inconel IN 738 LC refractory alloy.

γ/γ' lattice mismatch. The alloy maintains high strength properties at temperatures up to ∼800 °C due to structural rearrangements that occur during heating. In particular, the structural transformations manifest themselves in the heat capacity. The increase of heat absorption was attributed by Brooks *et al* [21] to equilibration of the short-range order in the γ-phase matrix in the temperature interval 500–700 °C.

Inconel alloy exhibits non-monotonic temperature dependences of the dynamic yield strength Y whose relatively slow decrease from room temperature towards a minimum at 550 °C gives place to an abrupt increase of Y, within the narrow 30–50 °C temperature interval, followed by a recovery of the minimum value of the yield strength. Figure 12 demonstrates that

(i) the temperature of the anomaly of the shock yield stress coincides with the temperature of the anomaly in the heat capacity, and
(ii) the yield stress anomaly is caused by the high strain rate; it is absent under quasi-static conditions.

In the two-phase superalloys the shear stress responsible for the dislocation motion is governed by the coherency stress resulting from the temperature-dependent misfit between the lattices of the phases. It is plausible to assume that the equilibration of the short-range order in the γ-matrix responsible for the heat capacity anomalies is accompanied by a sharp change of the lattice misfit, which, in turn, produces stress of opposite sign in the γ' particles and in the γ-matrix. This misfit stress impedes the dislocation motion through the γ/γ' interfaces and, thus, increases the yield stress of the material. The change of the lattice misfit may explain the anomalies observed in both the spall and the dynamic yield strength. The correlation between anomalies in the heat capacity and the sub-microsecond strength properties looks very intriguing and promising in the sense of understanding the nature of high-rate plastic flow.

6. Discussion

Even the first studies of the yield and strength properties of metals and alloys at elevated temperatures and very high strain rates of shock-wave tests disclosed new interesting phenomena which could be expected but had not been discussed previously. The data show that the influence of temperature on the yield stress at high strain rates may be opposite to that at low and moderate strain rates. New experiments confirmed different shock behaviour of pure metals and metal alloys at elevated temperatures. In general, the shock response of alloys does

not contradict the hypothesis that phonon friction is the dominant mechanism at high strain rates and temperatures. The transition from 'thermal softening' to 'thermal strengthening' depends on the strain rate, and occurs between 0.2 and 0.5 GPa of the yield stress. Observation of non-monotonic variations of the strength properties of complicated alloys should contribute to understanding their structural rearrangements at heating.

The dynamic tensile strengths of metal single crystals and polycrystalline metals exhibit different temperature dependences near the melting point that are treated in terms of superheating and pre-melting. The problem of the real mechanisms and kinetics of melting is still unsolved and attractive. Whereas superheated solid states are allowed by theory and have been observed in experiments, nothing is known about the mechanical and thermophysical properties of matter in these exotic metastable states, and about the real temperature and time limits of their existence. The presence of intergranular surfaces in polycrystalline material introduces a local distortion of the crystal lattice that results in pre-melting phenomena at temperatures below the bulk melting point.

Shock-wave experiments at elevated temperatures open new capabilities to study the fundamental strength properties of a matter, equations of state, polymorphic transformations and phase transitions under compression and tension. Future investigations in this direction promise interesting new data on metastable states and time-dependent processes which will undoubtedly help us to better understand the mechanisms and kinetics of plasticity, fracture, and structural transformations of solids.

References

[1] Clifton R J 1971 *Shock Waves and the Mechanical Properties of Solids* ed J J Burke and V Weiss (Syracuse, NY: Syracuse University Press) pp 73–116

[2] Bhate N, Clifton R J and Phillips R 2002 *Shock Compression of Condensed Matter—2001* ed M D Furnish *et al* (Melville, NY: American Institute of Physics) pp 339–42

[3] Mogilevsky M A and Mynkin I O 1978 *Combust. Explo. Shock Waves* **14** 159–63

[4] Curran D R, Seaman L and Shockey D A 1987 *Phys. Rep.* **147** 254–388

[5] Kanel G I, Razorenov S V, Bogatch A A, Utkin A V, Fortov V E and Grady D E 1996 *J. Appl. Phys.* **79** 8310–17

[6] Bogach A A, Kanel G I, Razorenov S V, Utkin A V, Protasova S G and Sursaeva V G 1998 *Phys. Solid State* **40** 1676–80

[7] Kanel G I, Razorenov S V, Baumung K and Singer J 2001 *J. Appl. Phys.* **90** 136–43

[8] Kanel G I, Razorenov S V, Baumung K and Bluhm H 2002 *Shock Compression of Condensed Matter—2001* ed M D Furnish *et al* (Melville, NY: American Institute of Physics) pp 603–6

[9] Antoun T, Seaman L, Curran D R, Kanel G I, Razorenov S V and Utkin A V 2003 *Spall Fracture* (New York: Springer)

[10] Barker L M and Hollenbach R E 1974 *J. Appl. Phys.* **45** 4872–87

[11] Kanel G I 1999 *Fatigue Fract. Eng. Mater. Struct.* **22** 1011–9

[12] Ubbelohde A R 1965 *Melting and Crystal Structure* (Oxford: Clarendon)

[13] Dash J D 1999 *Rev. Mod. Phys.* **71** 1737–43

[14] Lu J and Szpunar J A 1995 *Interface Sci.* **3** 143–50

[15] Razorenov S V, Kanel G I and Fortov V E 2003 *Phys. Met. Metallogr.* **95** 86–91

[16] Ninomura T 1974 *J. Phys. Soc. Japan* **36** 399

[17] Krüger L, Kanel G I, Razorenov S V, Meyer L and Bezruchko G S 2002 *Shock Compression of Condensed Matter—2001* ed M D Furnish *et al* (Melville, NY: American Institute of Physics) pp 1327–30

[18] Kanel G I, Razorenov S V, Zaretsky E B, Herrman B and Meyer L 2003 *Phys. Solid State* **45** 656–61

[19] Zwicker U 1974 *Titan und Titanlegierungen* (Berlin: Springer)

[20] Zaretsky E B, Kanel G I, Razorenov S V and Baumung K 2003 *Int. J. Impact Eng.* at press

[21] Brooks C R, Cash M and Garcia A 1978 *J. Nucl. Mater.* **78** 419–21

[22] Bettge D, Osterle W and Ziebs J 1995 *Z. Metalk.* **86** 190–7